Computers, Materials & Continua

Tech Science Press

https://doi.org/10.32604/cmc.2026.084415

ARTICLE

A Load-Balancing and Energy-Efficient Routing Protocol Based on Multi-Factor Ant Colony Optimization for WSNs

Kexin Liao[1], **Deyu Lin**[1,2,*], **Ran Hu**[1], **Yufei Zhao**[2] **and Yong Liang Guan**[2]

[1]School of Software, Nanchang University, Nanchang, China
[2]School of Electrical and Electronic Engineering, Nanyang Technological University, Singapore
*Corresponding Author: Deyu Lin. Email: dashing_lin@126.com

Received: 22 April 2026; Accepted: 14 July 2026; Published: 22 October 2026

ABSTRACT: The Wireless Sensor Networks (WSNs), serving as the perception layer of the Internet of Things (IoT), play a vital role in various fields such as environmental monitoring, smart homes, and industrial automation. However, the limited battery capacity of sensor nodes and the uneven traffic burden caused by multi-hop transmission often lead to premature node death, energy holes, and network partitioning. To address these problems, this paper proposes an Energy-efficient and Load-balanced Routing protocol based on Ant Colony optimization (ELRAC). First, a hierarchical regional network model and an angle-based neighbor pre-screening mechanism are designed to reduce ineffective node interactions and avoid backward or detoured forwarding. Second, a composite heuristic function integrating distance, directional angle, and residual energy is constructed to guide ants toward energy-efficient and load-balanced next-hop selection. Third, a dynamic pheromone replenishment mechanism is introduced to maintain route diversity and alleviate premature convergence. Simulation experiments are conducted under different network settings and compared with representative routing protocols, including LEACH, R-LEACH, GWOA-CH, and AEGWO-CH. The results show that ELRAC improves packet delivery, energy utilization, and overall routing stability while maintaining a balanced network lifetime. These results demonstrate that the proposed protocol can effectively enhance load balancing and energy-efficient routing performance in WSNs.

KEYWORDS: Wireless sensor networks; routing; ant colony optimization; network lifetime; load balancing

1 Introduction

In recent years, with the rapid advancement of the Internet of Things (IoT) and intelligent sensing technologies [1], Wireless Sensor Networks (WSNs) have gained significant importance, serving as a critical bridge connecting the physical and digital worlds [2]. Leveraging the self-organizing, low-cost, and wide-area coverage characteristics, WSNs have become important in numerous fields, such as environmental monitoring [3], industrial automation [4], and precision agriculture [5]. In traditional WSNs, sensor nodes are typically powered by batteries with limited energy capacity and are often deployed in harsh environments where it is difficult to access, and energy replenishment is exceptionally challenging. Consequently, how to maximize the network lifetime and the Quality of Service (QoS) remains one of the most fundamental challenges in the field of WSNs. Actually, the network lifetime is directly determined by the efficiency and balance of energy consumption. Over the past decades, extensive research has investigated approaches to improving the energy efficiency of WSNs, including routing optimization [6] and data compression for efficient transmission [7]. Among various solutions, the optimization of routing protocols is widely

Copyright © 2026 The Authors. Published by Tech Science Press. This work is licensed under a Creative Commons Attribution 4.0 International License, which permits unrestricted use, distribution, and reproduction in any medium, provided the original work is properly cited.

recognized as a pivotal method for enhancing the energy efficiency of WSNs. However, traditional routing algorithms tend to favor shortest-path selection, which often leads to premature energy depletion of critical nodes due to excessive data forwarding tasks, ultimately resulting in network partitioning and severe performance degradation.

To address the aforementioned challenges, nature-inspired metaheuristic algorithms, particularly Ant Colony Optimization (ACO), have been extensively introduced into WSN routing design due to their capability in solving complex path optimization problems [8,9]. By simulating the pheromone-based positive feedback mechanism of ant colonies, ACO can dynamically discover and approach the optimal path. Nonetheless, classical ACO routing algorithms still exhibit notable limitations in WSNs: Firstly, their heuristic function typically considers only the inter-node distance, lacking comprehensive consideration of energy status and transmission direction, making them prone to falling into local optima. Secondly, during the initial route establishment phase, nodes require extensive control message exchanges to explore paths, generating substantial unnecessary communication overhead. Thirdly, the conventional pheromone update mechanism easily leads to premature convergence of the algorithm, restricting its ability to find global optimal solutions in dynamic network environments.

To this end, a load-balanced and energy-efficient routing protocol based on an improved ant colony optimization is proposed in this paper. Specifically, the main contributions of this work can be summarized as follows,

(1) A hierarchical regional network model is proposed, along with a neighbor node pre-screening mechanism incorporating an angle factor, this mechanism leverages an angle factor to strategically confine the communication range for route discovery, effectively filtering out neighbors that would lead to backward or detoured paths, thereby significantly reducing control overhead and energy consumption during route establishment,
(2) A composite heuristic function integrating distance, angle, and energy factors has been designed, which is able to dynamically balance transmission distance, directional guidance, and node residual energy, thereby steering route selection toward energy efficiency and load balancing,
(3) A dynamic replenishment pheromone update mechanism is introduced as a route maintenance strategy. By implementing a minimum pheromone concentration threshold and a stochastic replenishment strategy, it mechanism effectively prevents premature algorithm stagnation, enhances the exploration capability for global optimal paths, and improves the protocol's robustness.
(4) Simulation experiments demonstrate that the proposed protocol significantly outperforms existing schemes (e.g., Low Energy Adaptive Clustering Hierarchy (LEACH), residual-energy-based LEACH (R-LEACH), and Grey Wolf Optimization and Whale Optimization Algorithm-based cluster-head selection (GWOA-CH)) in terms of network lifetime, throughput, and energy efficiency, thereby validating its practical effectiveness.

The remainder of this paper is organized as follows. Section 2 reviews related works, followed by Section 3, in which the system model and problem definition is elaborated. Section 4 presents analytical proofs of relevant theories and mechanisms. Section 5 details the design specifics of the proposed routing protocol. The experiments and result analysis are presented in Section 6. Finally, we draw the conclusion and outline some potential future research directions.

2 Related Works

Recent studies have investigated WSNs from different perspectives, including mobile energy replenishment, battery-free data collection, underwater sensing, traffic-load-aware resource management, reliability

evaluation, QoS-aware routing, and Unmanned Aerial Vehicle (UAV)-assisted data collection [10]. Mobile energy replenishment and battery-free scheduling have been studied to alleviate the energy limitation of sensor nodes [11,12]. Underwater WSNs introduce additional challenges such as restricted transmission, unreliable links, and traffic-load variation [13,14]. In addition, trust management [15], deep reinforcement learning, graph neural networks [16], and machine-learning-based routing [17] have been introduced to improve security, reliability, and QoS in WSNs. These studies indicate that energy limitation, load balancing, and reliable data forwarding remain key challenges in practical WSN deployments.

Improving energy efficiency and extending the lifetime of Wireless Sensor Networks (WSNs) remain important challenges in the field [18]. To address this issue, researchers have primarily focused on the optimization of network architecture and routing protocols [19]. Among these, clustering-based protocols and metaheuristic optimization methods have been widely investigated for improving energy efficiency and extending network lifetime [20,21].

Clustering is an effective and widely adopted energy-saving technique [22]. Its core concept involves organizing the network into a cluster-based structure, where Cluster Heads (CHs) are responsible for data aggregation and long-distance transmission, thereby reducing the energy consumption associated with nodes communicating directly with the Sink. The Low Energy Adaptive Clustering Hierarchy (LEACH) protocol is a pioneering work in this field [23]. By randomly rotating the role of cluster heads, LEACH distributes the network's energy consumption evenly across all sensor nodes, thereby preventing fixed CHs from depleting their energy too rapidly. However, since the process of the Cluster Head selection is entirely random and does not consider the residual energy or geographical location of the nodes, the nodes with lower energy are easily to be selected as CHs and use up their energy prematurely, and may also result in an uneven distribution of cluster heads. To address these issues, the R-LEACH algorithm was proposed [24], in which the node's initial energy and the residual energy are adopted as key parameters in the cluster head election process, thus allowing nodes with higher energy a greater chance of becoming cluster heads. As a result, the balance of the network load can be significantly improved.

To identify globally optimal paths or cluster head deployments in more complex network environments, researchers have introduced various metaheuristic algorithms, thereby establishing an important research direction in intelligence-based optimization routing protocols.

The Particle Swarm Optimization-based Energy-efficient Cluster Head Selection (PSOECHS) algorithm leverages the global search capability of PSO to select the proper CH [25]. During the process of Cluster Head election, it comprehensively considers inter-node distances, the distance from nodes to the Sink, and the residual energy of nodes, thus promoting the formation of cluster structures with superior energy efficiency and geographically balanced. Similarly, Loganathan and Arumugam proposed the ECPSO algorithm [26], in which not only PSO was adopted for cluster head selection but also new roles, i.e., assistant Cluster Heads and super Cluster Heads, are innovatively introduced for each cluster, with the former handling data aggregation and the latter managing communication with the Sink. This design effectively distributes the workload traditionally handled by a single cluster head, further delaying the energy depletion of Cluster Heads. GWOA-CH, a dual-cluster-head hierarchical routing protocol, combines Grey Wolf Optimization (GWO) and the Whale Optimization Algorithm (WOA) for cluster-head selection [27]. By considering the residual energy of sensor nodes and their distances to the Sink, it aims to achieve more balanced network energy consumption. Furthermore, the Energy-Aware Hybrid Approach (EAHA) incorporates genetic algorithms to optimize the selection of multi-hop routing paths [28]. By identifying the path with the lowest energy consumption among candidate paths and striving to achieve energy balance among nodes, the network lifetime can be effectively prolonged.

In summary, existing research has made remarkable progress in enhancing the energy efficiency and balancing network load of WSNs through the introduction of metaheuristic algorithms and the optimization of network architectures. However, as Internet of Things application scenarios grow increasingly complex, these solutions still face challenges in adapting to dynamic network environments. These metaheuristic-based routing protocols remain constrained by two critical bottlenecks in practical deployment. Firstly, in the route discovery phase, the global information interactions necessary for route evaluation—such as the fitness calculations in PSO and GWO algorithms—consume the very energy intended to be saved, which fundamentally contradicts the core objective of these protocols. Secondly, the persistent risk of premature convergence poses a particularly critical issue for ACO-based schemes, where imbalanced pheromone distribution can easily trap the algorithm in local optima, preventing it from identifying globally optimal routing paths throughout the network's operational lifetime. Consequently, the fundamental challenge of significantly reducing control overhead while simultaneously ensuring robust exploratory capability to escape local optima remains a pivotal and non-trivial problem. To address these challenges, this paper proposes the Energy-efficient and Load-balanced Routing protocol based on Ant Colony optimization (ELRAC), which incorporates a hierarchical network model, a neighbor pre-screening mechanism, and a dynamic pheromone update strategy to sustain performance gains in both energy efficiency and network lifetime. For the sake of convenience, the comparisons on the existing technologies and our main concerns are listed in Table 1.

Table 1: Comparisons on the existing technologies and our main concerns.

Categories	References	Advantage	Disadvantage
Cluster-based Routing Protocols	[22–24]	Balances network energy consumption through cluster-head rotation; simple structure with good scalability.	Random cluster-head selection does not consider node residual energy or location, easily leading to load imbalance and premature node death.
Metaheuristic Optimization-based Protocols	[25–28]	Possesses global search capability, dynamically finding near-optimal paths; suitable for complex optimization problems.	High control overhead during route establishment; The pheromone update mechanism is prone to premature convergence, trapping the algorithm in local optima.
Our main concerns	1. A neighbor node pre-screening mechanism to restrict ineffective interactions and reduce overhead. 2. A composite heuristic function integrating distance, angle, and energy to achieve load balancing and energy awareness. 3. A dynamic replenishment pheromone update mechanism to prevent premature convergence and enhance global search capability.		

3 System Model

In this section, a hierarchical network model is presented. Subsequently, the energy consumption model is illustrated, and the relationship among energy consumption and communication distance, data traffic volume is also pointed out. Finally, the definitions concerning the relevant concepts are detailed and the specific mathematical expressions are presented at length.

3.1 Hierarchical Network Model

A hierarchical network model is proposed in this paper. The entire network is divided into unequal ring-shaped regions based on the hierarchical regional data volume dissemination feature as well as the energy consumption model. As shown in Fig. 1, each sensor node is assigned a specific level ID, which is adopted to promote energy equilibrium between adjacent levels. Actually, the hierarchical network model is utilized to construct the routing table based on the optimized ant colony algorithm, thus establishing an optimal routing from the source to the Sink. For simplicity, the hierarchical network topology is only built during the phase of network initialization and keeps fixed.

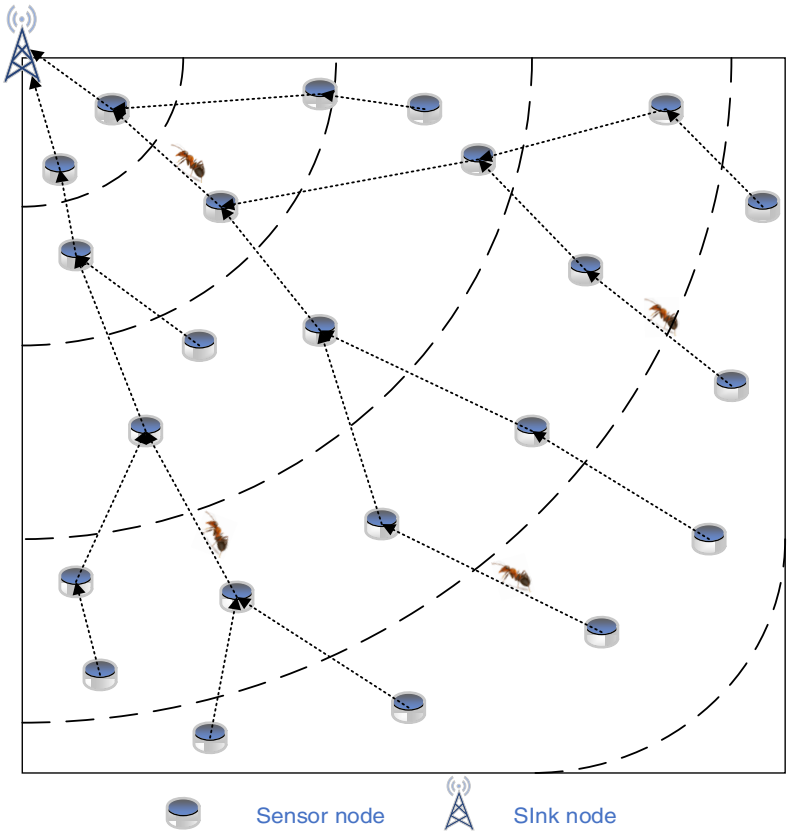


Figure 1: Hierarchical network model.

3.2 Energy Consumption Model

In this paper, the first-order radio model is adopted to describe energy consumption for data transmission. To be specific, the energy consumed by a sensor node's transmission per k bits of data over a distance of d is mathematically expressed below,

$$E_{tx} = k \times E_{elec} + k \times \varepsilon_{amp} \times d^{l} \tag{1}$$

where E_{elec} denotes the energy consumed to receive or transmit per bit of data, and ε_{amp} is the Energy Loss Factor for amplifier circuits, generally defined as 10 pJ/bit/m^2; d denotes the communication distance between the source and the destination, l is the attenuation coefficient ranging from 2 to 4. In general, the value of l is related to the transmission mode [29].

The energy for sensor nodes to receive k bits data is mathematically expressed as below,

$$E_{rx} = k \times E_{elec} \tag{2}$$

According to Eqs. (1) and (2), the total energy consumption of sensor nodes for communication can be expressed as follows,

$$E = E_{tx} + E_{rx} \tag{3}$$

3.3 Relevant Definitions

To achieve the optimized energy-efficient routing in WSNs, the effects of path, angle, and energy factors on routing decision-making are considered comprehensively. The relevant definitions of are proposed for analysis.

3.3.1 Angle Factor

As shown in Fig. 2, s denotes the Sink; i is the current node, and j, j_1 are the feasible candidates for the next hop. The angle of $\angle sij$ denotes the angle factor, which is used for routing guidance. To be specific, the angle factor can be mathematically expressed as follows,

$$\theta_{sij} = arccos\frac{{d_{si}}^2 + {d_{ij}}^2 - {d_{sj}}^2}{2 \times d_{si} \times d_{ij}} \tag{4}$$

where θ_{sij} denotes the angle of $\angle sij$, d_{si} denotes the distance between the current node and the Sink, d_{ij} denotes the distance between the current node i and the next hop node j, and d_{sj} denotes that between the Sink s and the next hop j.

3.3.2 Pre-Screening Range of Neighbor Nodes

As shown in Fig. 3, the definition of pre-screening range of neighbor nodes, which is referred as the communication range of nodes in this paper, is proposed to reduce the amount of information interaction of nodes. The valid communication range of nodes is set to cut down the extra energy consumption during the network initialization phase. Specifically, the pre-screening range of neighbor nodes can be mathematically defined as follows,

$$U_i = \{j | d_{ij} < H_{\max} \cap \theta_{sij} < 90^\circ\} \tag{5}$$

where U_i is the set of nodes within the pre-screening range of node i. It can also be expressed as the set of nodes locating in the communication range of node i. d_{ij} denotes the distance between node i and node j. $H_{\max}$ is the maximum communication range of node i and θ_{sij} is the angle of $\angle sij$. Specifically, $H_{\max}$ is defined mathematically below,

$$H_{\max} = \begin{cases} dt_i, Sum(U_i) > 0 \\ dt_i + 1, Sum(U_i) <= 0 \end{cases} \tag{6}$$

where dt_i denotes the width of the hierarchical region where node i locates. Actually, it is the valid communication range of node i. $Sum(U_i)$ denotes the number of nodes that can communicate effectively with node i. If there is no feasible next-hop available within the valid communication range of the current node, $H_{\max}$ is incremented in size until a feasible next-hop appears.

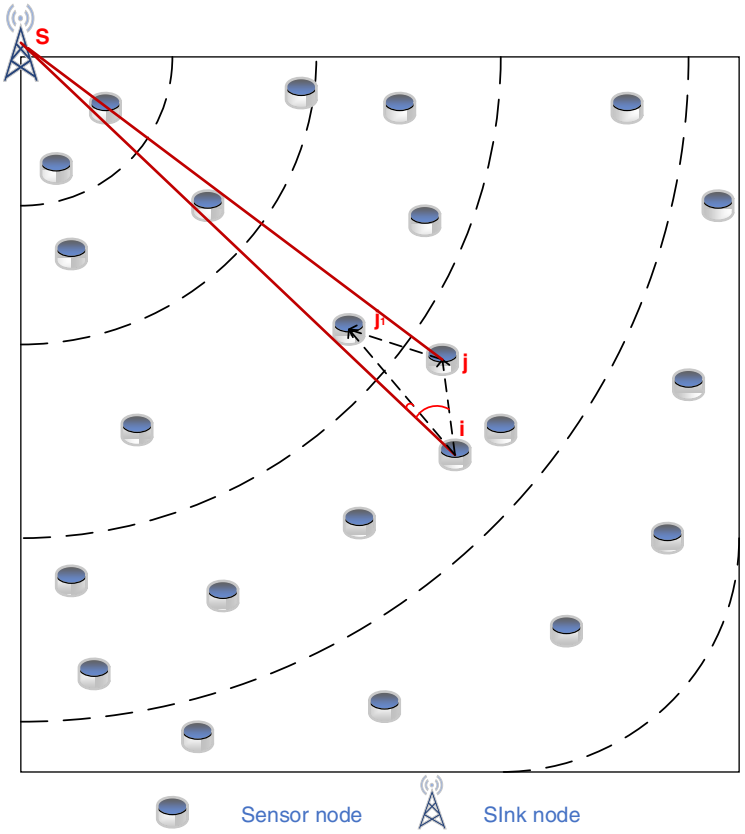


Figure 2: Diagram of the angle factor.

3.3.3 Energy Factor

Since the node's residual energy helps to avoid network communication interruptions due to energy depletion, a novel concept of Energy Factor (EF, which is shown in Fig. 4) is proposed in this paper, which is utilized to measure the data propagation ability of sensor nodes. To be specific, the mathematical definition of EF is presented as follows,

$$EF = EV_i - E_i \tag{7}$$

here, the Energy Factor (EF) represents the Energy Safety Margin of node i. By subtracting the predicted energy consumption (E_i) from the residual energy (EV_i), EF evaluates whether a node has a sufficient power buffer to undertake the upcoming data forwarding task. A larger EF indicates a higher load-bearing capability. To avoid energy depletion, if $EF <= 0$, node i is considered to have insufficient energy and will be temporarily excluded from the feasible next-hop candidate set, thus effectively preventing the emergence of energy holes.

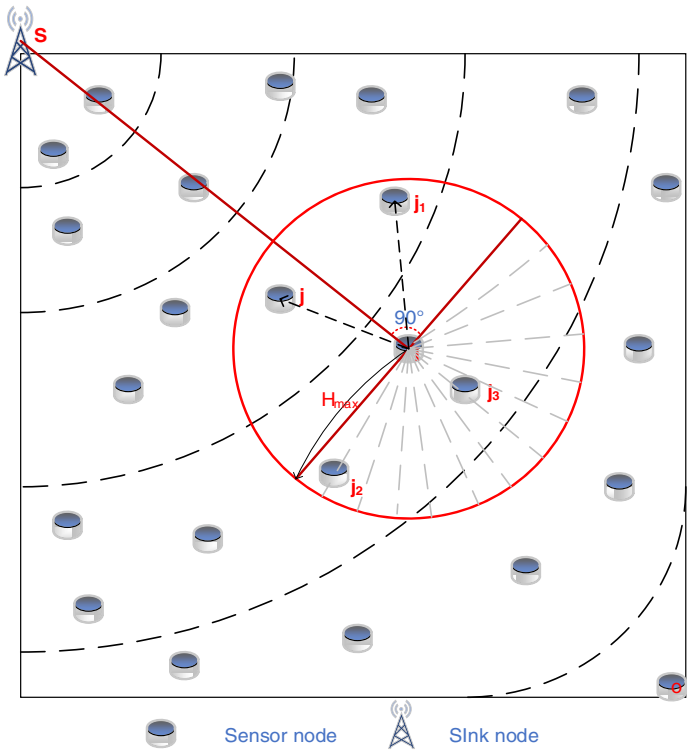


Figure 3: Neighborhood node pre-screening.

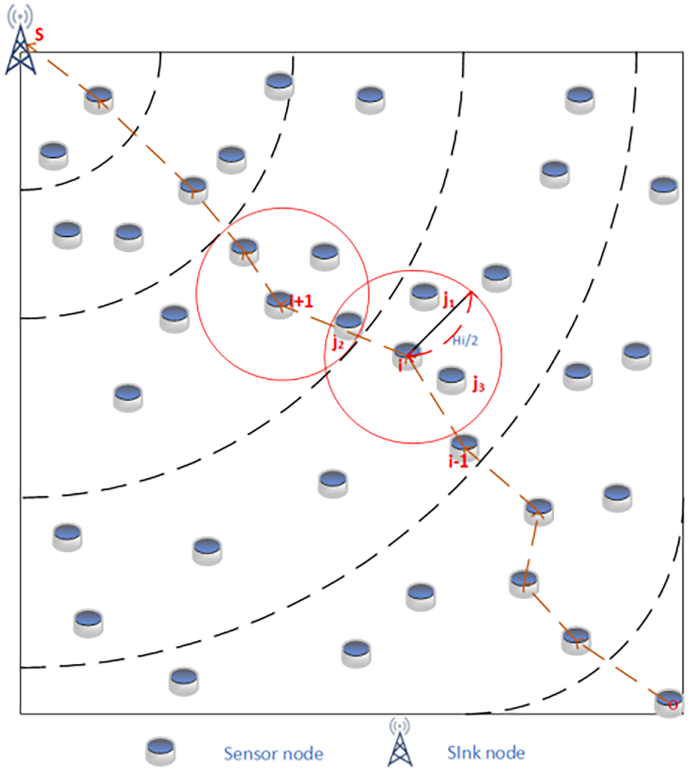


Figure 4: Schematic diagram of energy factor.

To obtain the value of E_i, it is necessary to compute the total amount of data propagated by node i ($Data_i$) firstly. The data transmitted by node i consists of the data forwarded from the previous hop, the data received from neighboring nodes, and the data generated by node i itself. It can be mathematically expressed as follows,

$$Data_i = Data_{i-1} + Cdata_i + kData \tag{8}$$

where $Data_{i-1}$ denotes the amount of data propagated by the previous hop node of node i. The value is obtained through message interactions among the sensor nodes, and $Cdata_i$ is the total amount of data propagated by other nodes to node i within the radius of $H_i/2$, centered at node i. $kData$ denotes the packet size propagated by an arbitrary node at a fixed time interval. To be specific, $Cdata_i$ can be expressed as follows,

$$Cdata_i = kData \times num_i \tag{9}$$

where num_i denotes the number of nodes located within the radius of $H_i/2$ from node i. Furthermore, since a sensor node does not need to receive the data it generates itself, the expected amount of received data for node i is $(Data_i - kData)$. By combining Eqs. (1)–(3), (8) and (9), the specific mathematical equation for the predicted energy consumption E_i can be obtained as follows,

$$E_i = (Data_i \times 2 - kData) \times E_{elec} + Data_i \times \varepsilon_{amp} \times {H_i}^l \tag{10}$$

4 Theoretical Analysis

In this section, the pre-screening mechanism of neighbor nodes, the mechanisms of route discovery and routing-pheromone update are elaborated. In addition, the relevant conclusions and definitions are proven and derived in detail.

4.1 Neighborhood Node Pre-Screening Mechanism

During the phase of network initialization, the valid communication range of nodes is set according to the neighboring node pre-screening mechanism, with the aim of avoiding extra energy consumption caused by invalid interactions. To be specific, neighbor node pre-screening, restricts the effective communication range of nodes based on the network hierarchy model and the angle factor, thereby ensuring a balance in network energy consumption. At the same time, this mechanism largely reduces the energy consumption of nodes for information interaction in the phase of route discovery.

4.1.1 Proof and Derivation of the Angle Factor

As shown in Fig. 2, according to the cosine theorem, it can be obtained that the three sides of Δsij and $\angle sij$ need to satisfy the following relation,

$${d_{sj}}^2 = {d_{ij}}^2 + {d_{si}}^2 - 2 \times d_{si} \times d_{ij} \times \cos\theta_{sij} \tag{11}$$

According to the definition of the inverse cosine function in trigonometry, we have:

$$y = \arccos(x) \tag{12}$$

where y denotes the required angle and x denotes the cosine value corresponding to the angle sought. Combined with Eqs. (11) and (12), the angle factor can be obtained by the following Expression,

$$\theta_{sij} = \arccos \frac{{d_{si}}^2 + {d_{ij}}^2 - {d_{sj}}^2}{2 \times d_{si} \times d_{ij}} \tag{13}$$

Lemma 1: *The introduction of angle factors contributes to the reduction in energy consumption.*

Proof: As shown in Fig. 2, the feasible next hop that can be selected by the current node i are node j and node j_1. The residual energy of node j is the same as that of node j_1. In traditional ant colony algorithms, the distance between two adjacent nodes is usually adopted as the selection criterion of the feasible next hop. In such a case, node i is more likely to choose node j as the next hop since it has a shorter distance. When node j makes routing decisions, according to the formula concerning the next hop probability selection in the ant colony routing algorithm, j_1 will be selected as the next hop. However, this route may introduce an unnecessary detour from node i to the Sink. In contrast, when the angle factor is introduced, the routing decision no longer depends only on the inter-node distance. The angle factor evaluates the directional alignment between each candidate node and the Sink. Since the pre-screening mechanism restricts candidate nodes to $\theta_{sij} < 90°$, a smaller θ_{sij} indicates that the candidate node is more consistent with the forwarding direction toward the Sink. In the improved heuristic function, this directional advantage is represented by $\cos\theta_{sij}$, where a smaller angle produces a larger cosine value and therefore a higher routing preference after normalization. Consequently, when node j_1 has a better directional alignment than node j under the same residual-energy condition, node i is more likely to select node j_1 as the next hop. This selection helps avoid backward or detoured forwarding and reduces unnecessary intermediate transmissions. According to Eqs. (1)–(3), communication energy consumption increases with transmission distance and data forwarding workload. Therefore, reducing detours and unnecessary relays can lower energy consumption and alleviate load imbalance. Thus, incorporating the angle factor into the heuristic function $n_{ij}(t)$ of the ant colony algorithm can reduce energy consumption and improve routing efficiency. □

4.1.2 Derivation and Proof of the Formula for the Width of the Graded Area of the Network Model

As shown in Fig. 5, assume the number of sensor nodes in the network is N. The distribution of sensor nodes follows a uniform distribution. The nodes send one unit of data volume per moment, according to the network data volume model, the total data received by the nodes per moment at level i can be expressed by the following equation,

$$Rdata_i = N \times \left(1 - \frac{(\sum_{j=1}^{i} d_j)^2}{L^2}\right) \tag{14}$$

where L denotes the distance from the boundary node o to the source node s; d_j represents the width of the region with partition level number j. Similarly, the total amount of data sent by nodes at level i can be denoted as follows.

$$Tdata_i = N \times \left(1 - \frac{(\sum_{j=1}^{i-1} d_j)^2}{L^2}\right) \tag{15}$$

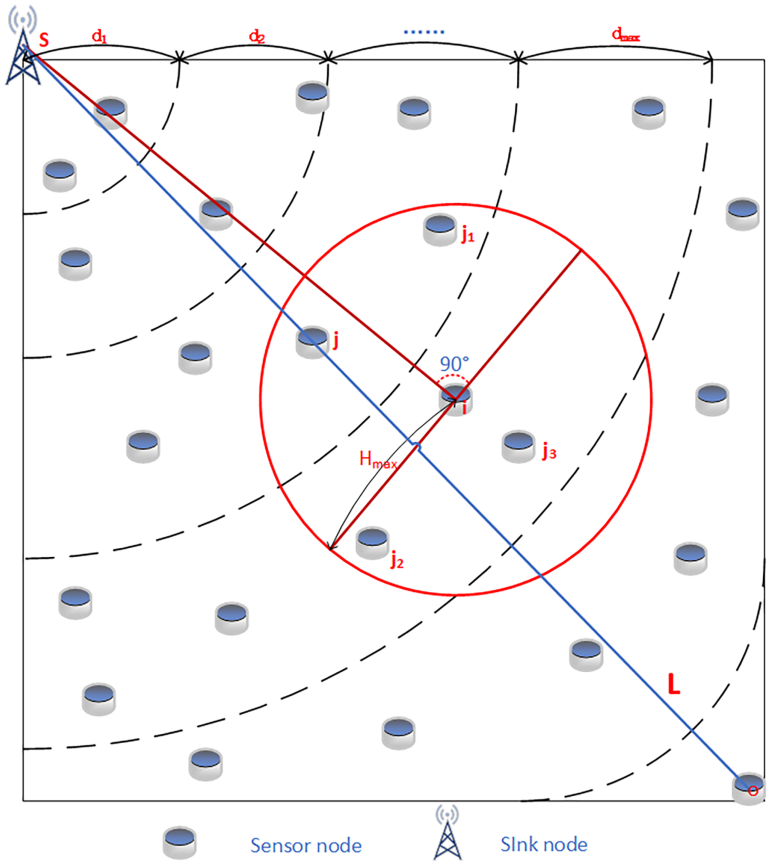


Figure 5: Schematic diagram of the grading network.

To balance the energy consumption between the graded zones, the following conditions need to be satisfied,

$$\begin{cases} E_1 = E_2 =, \ldots, = E_i \\ d_1 + d_2 + \ldots + d_i <= L \end{cases} \tag{16}$$

where E_i denotes the total energy consumption of the node at level i, and d_i is width of the region with partition level number i. Combine Eqs. (3), (14) and (15), and substitute the equations shown in Eq. (16), the width of each graded region can be solved to achieve energy balance among the sensor nodes in the graded region. It is actually the maximum effective communication distance of the sensor nodes corresponding to the graded region number defined in this paper. Theoretical analysis indicates that the adoption of the network graded area width as the effective communication distance of the nodes ensures the energy consumption balance between areas to a large extent and reduces the average energy consumption level of the nodes during the formation of the network route.

Lemma 2: *Pre-screening of neighboring nodes can effectively reduce the extra energy consumption during the phase of the network initialization.*

Proof: As shown in Fig. 5, the current node i forms a circular region with a radius of $H_{\max}$, which represents the effective communication range of node i. Accordingly, the set of next hops of node i can be derived as $\{j, j_1, j_2, j_3\}$. It can be found that if nodes j_2 and j_3 are chosen, the total length of the network routing path

will increase to some extent. It leads to an increase in the average energy consumption of sensor nodes, which further results in energy unbalance for the whole network. On the contrary, the neighbor node pre-screening mechanism mentioned in this paper can filter out both nodes that lie beyond the preset communication range and those within the range that are deemed unsuitable for interaction, such as nodes j_2 and j_3. In summary, the introduction of the neighbor node pre-screening mechanism can effectively avoid invalid information interaction among nodes during the network initialization phase, which largely reduces energy consumption. □

4.2 Route Discovery Mechanism Based on Improved Heuristic Function

In WSNs, routing metrics play a critical role in determining the next hop. Traditional ant colony algorithms typically rely solely on inter-node distance as heuristic information, which often leads to energy imbalance and local optimum issues. To establish a more intelligent and balanced routing mechanism, a multi-dimensional routing metric that comprehensively considers three key factors (namely distance, angle, and energy) is presented, thus enabling a holistic evaluation of candidate path quality.

Consider a practical scenario where a sensor node needs to select the next hop from multiple candidate nodes. As shown in Fig. 6, when node A needs to transmit data to the Sink, it has three candidate next hops, B, C, and D. In traditional approaches based solely on distance, node B would typically be selected as it is closest to A. However, B might become an energy hole due to its excessive data forwarding tasks. Under our composite metric framework, the selection process becomes more sophisticated: while node B has the best distance factor, node C has a more favorable angular position relative to the Sink (smaller θ_{sij}), and node D possesses significantly higher residual energy. The comprehensive evaluation of these three dimensions ensures the selection of a holistically optimal candidate, rather than one that is merely geographically optimal.

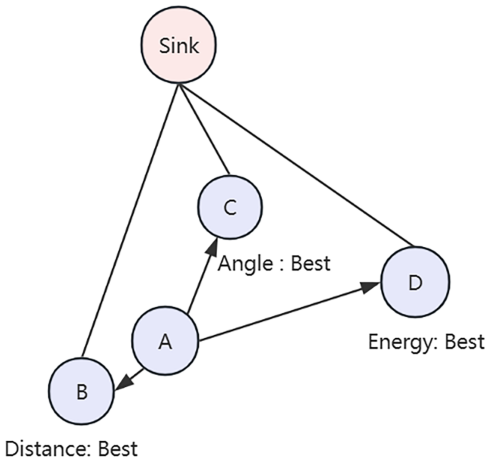


Figure 6: An illustrative scenario of multi-factor routing decision.

This composite routing metric mechanism comprises three core elements: the distance factor $Eta(i, j)$, which reflects communication energy consumption by calculating the reciprocal of inter-node distance, thereby promoting the establishment of energy-efficient transmission paths; the angle factor θ_{sij} which evaluates the directional deviation of candidate nodes relative to the Sink, thus effectively preventing detours during data transmission; and the energy factor EF which dynamically assesses nodes' load capacity by comparing their residual energy with predicted consumption, thus preventing the formation of energy hotspots. These three elements work in concert to guide routing selections toward achieving minimal energy consumption, optimal directionality, and the most balanced load distribution.

Based on this composite routing metric mechanism, this paper refines and restructures the heuristic function of the traditional ant colony algorithm into a new form that incorporates distance, angle, and energy factors.

However, it is crucial to note that the three components—distance, angle, and energy—possess fundamentally different numerical scales. If used as raw values, the factor with the largest absolute value may dominate the heuristic calculation, significantly reducing the intended multi-factor balance. To address this issue, we employ Min-Max normalization within the current feasible candidate set (denoted as Allow) to map all three metrics into a uniform dimensionless scale of [0, 1].

Furthermore, instead of using the raw angle θ_{sij}, we utilize $\cos(\theta_{sij})$. Since the pre-screening mechanism strictly limits the angle to $\theta_{sij} < 90°$, a smaller angle (indicating a better directional alignment toward the Sink) naturally yields a larger cosine value approaching 1, which strictly aligns with the positive feedback requirement of the routing probability.

For any candidate node j in Allow, the normalized factors are calculated as follows:

$$\begin{cases} \text{Norm}\left(n_{ij}\right) = \dfrac{n_{ij} - \min(n)}{\max(n) - \min(n) + \varepsilon} \\ \text{Norm}\left(Angle_{ij}\right) = \dfrac{\cos(\theta_{sij}) - \min(\cos(\theta))}{\max\left(\cos(\theta)\right) - \min\left(\cos(\theta)\right) + \varepsilon} \\ \text{Norm}\left(EF_j\right) = \dfrac{EF_j - \min(EF)}{\max\left(EF\right) - \min\left(EF\right) + \varepsilon} \end{cases} \tag{17}$$

where n_{ij} denotes the reciprocal of the distance between node i and j, ε is a remarkably small constant introduced to prevent division by zero, and min(.) and max(.) represent the extreme values within the current Allow set.

Consequently, the improved heuristic function is strictly governed by the designated weight parameters, defined mathematically below:

$$n_{ij}(t) = \left[\text{Norm}\left(n_{ij}\right)\right]^{\alpha} \times \left[\text{Norm}\left(Angle_{ij}\right)\right]^{\beta} \times \left[\text{Norm}\left(EF_j\right)\right]^{\gamma} \tag{18}$$

α denotes the weight of the distance decision factor; β denotes the weight of the angle decision factor; and γ denotes the weight of the energy decision factor. The improved heuristic function incorporates energy and angle factors, which guides the path selection towards paths that consist of energy-rich nodes and have shorter geometric lengths**.** It directly promotes load balancing and extends network lifetime. To determine the weighting parameters, the settings of the distance and energy weights, α and γ, were informed by the energy-efficient Ant Colony System presented by Xia et al. [9], which highlights the importance of jointly considering transmission distance and energy status in WSN routing. Since the angle factor is newly incorporated into the heuristic function of ELRAC, its weight β cannot be directly adopted from the above study. Therefore, the final values of α, β, and γ were determined through the parameter sensitivity analysis presented in Section 6.2.7, based on the overall trade-off among network lifetime, packet delivery, energy efficiency, and routing stability.

4.3 Dynamic Replenishment-Based Pheromone Update Mechanism for Routing

In this section, a new pheromone update mechanism is proposed to guarantee reasonable positive feedback by supplementing and volatilizing the pheromones on the path to different degrees. Meanwhile, it can also avoid premature convergence of the algorithm caused by premature pheromone accumulation

and reduce the risk of route exploration failing to reach the global optimum. To be specific, the pheromone update approach can be denoted by the following expression,

$$tau\,(i,j) = \begin{cases} (1-Rho1) \times tau(i,j) + Ptau(i,j), Ptau(i,j)! = 0 \\ (1-Rho2) \times tau(i,j), Ptau(i,j) = 0 \\ (1+Rho3)^{ri} \times tau(i,j), tau(i,j) < T_{min} \end{cases} \tag{19}$$

where $tau(i,j)$ denotes the pheromone concentration from node i to node j, $Ptau(i,j)$ denotes the pheromone increment from node i to node j after one round of path exploration iteration, $Rho1$ denotes the pheromone volatilization rate factor in case that the pheromone increment is not zero, $Rho2$ denotes the pheromone volatilization rate factor in case that the pheromone increment is zero; $T_{\min}$ denotes the set minimum pheromone threshold, $Rho3$ denotes the pheromone concentration replenishment rate between nodes after the pheromone concentration falls below the minimum threshold. Assume ri denotes the number of pheromone replenishments, defined as follows,

$$ri = randi(Min, Max) \tag{20}$$

where $randi(\cdot)$ is a random number function, Min denotes the set minimum threshold for the number of pheromone replenishments, and Max denotes the set maximum threshold for the number of pheromone replenishments.

The key is the third case in Eq. (19): if $tau(i,j) < T_{\min}$, then $tau(i,j) = (1+Rho3)^{ri} \times tau(i,j)$. Since $Rho3 > 0$ and $ri \geq 1$, $(1+Rho3)^{ri} > 1$. It ensures no pheromone trail ever decays to zero permanently. Thus, all edges maintain a non-zero probability of being explored, preventing the algorithm from completely abandoning any potential path and succumbing to local optima.

5 Load Balancing Energy Efficient Routing Protocol Based on Ant Colony Algorithm

In this section, an Energy-efficient Load-balanced Routing algorithm based on Ant Colony (ELRAC) optimization for WSNs is proposed in this section. The detailed algorithmic description of the implementation process for each stage of route construction is presented below.

5.1 Overview of Protocol

The algorithm mainly consists of three phases, namely the network initialization phase, the route discovery phase, and the pheromone update phase, respectively. In the network initialization phase, a hierarchical network model and the angle factor are utilized to pre-screen the neighboring nodes, with the aim to avoid invalid information interaction among sensor nodes and save the energy consumption. In the route discovery phase, the heuristic function is improved by combining both the residual energy of the nodes and the exploration angle, which is used to select the most suitable next hop. In the pheromone update phase, the improved pheromone update approach alleviates premature convergence and mitigates the local optimum problem in the route discovery phase, further guaranteeing the energy balance of the whole network. To be specific, the algorithm of ELRAC is listed as shown in Algorithm 1.

Algorithm 1: ELRAC pseudocode

INPUT: M: Ant collection, N:Collection of sensor nodes
OUTPUT: Find the optimal route from the source node to the destination node
1: Initialize network model related parameters
2: **while** ¬ Reach the maximum number of iterations **do**

(Continued)

Algorithm 1 (continued)

3: Initialize the ant's path information table
4: **for** m_i ← 1 to M **do**
5: **for** n_i ← 1 to N **do**
6: Calculate the pre-screening range of neighboring nodes in the ant route exploration process, go to Algorithm 2
7: Calculate the selection probability of the node, select the next hop of the route and go to Algorithm 3
8: **end for**
9: **end for**
10: Calculate path length: Length_i
11: Update the pheromone on the routing path to Algorithm 4
12: Reinitialize the path information table to empty
13: Number of iterations plus one
14:**end while**

5.2 Details of ELRAC

5.2.1 Network Initialization Phase

In the traditional ant colony routing algorithm, when the next hop node is selected, information interactions are made with other nodes to obtain information, such as node distance and node energy. However, most of these interactions are ineffective, owing to the large energy consumption of the nodes. To address this problem, a neighbor node pre-screening algorithm is proposed in this paper. To be specific, the candidate set of nodes to be visited is determined firstly based on the sequence of nodes already visited by the ant. Then the candidate nodes are screened by combining the node's hierarchical region code and the angle factor, eliminating those that do not meet the communication range or angle conditions. If the candidate set is empty, the communication range is adaptively expanded. Through this process, it effectively reduces the invalid information interactions between nodes, thereby minimizing extra energy consumption during the network initialization phase. The details are described in Algorithm 2.

Algorithm 2: Neighborhood node pre-screening pseudocode

INPUT: Table: Ant's path information table, D(i, j): Network node distance information table,
Locate: Node area code information table, Nodeindex: Node Sequence, Radiu: Network grading distance information table
OUTPUT: Find the set of nodes to be visited by ants
1: Calculate the set of nodes to be visited by ants: $Visited = Table(m_i, 1{:}(n_i - 1))$
2: Compute the set of unvisited nodes of ants: $AllowNode =\sim ismember(Nodeindex, Visited)$
3: **for** z_i ← 1 to N **do**
4: Get the current node: $CurrentNode = Table(m_i, n_i - 1)$
5: Get the node's level number: $BlockNum = Locate\,(CurrentNode)$
6: Calculate the angle factor according to the angle factor formula: θ
7: **if** θ >= 90 || D(CurrentNode, z_i) > Radiu(BlockNum) **do**
8: Settings the set of unvisited nodes of ants: $AllowNode(z_i) = 0$
9: **end if**
10: **end for**

(Continued)

Algorithm 2 (continued)

11: **if** the set of unvisited nodes of ants is null **do**
12: Increase the access radius, as in the above step to reacquire the generation access node combination of ants
13: **end if**
14:Get the set of unvisited nodes of ants: $Allow = Nodeindex(AllowNode)$

In Algorithm 2, the neighbor node pre-screening process primarily involves node set operations and conditional judgments in terms of time complexity. The algorithm first computes the sets of visited and unvisited nodes, through an operation with a time complexity of $O(N)$. It then iterates through each node in the network, performing distance calculations, angle factor computations, and communication range condition checks. This loop executes N times, resulting in a time complexity of $O(N)$. In terms of space complexity, the algorithm needs to maintain the sets of visited and unvisited nodes, each occupying $O(N)$ space, while also storing temporary variables required for angle factor calculations, leading to a space complexity of $O(N)$. In summary, Algorithm 2 has a time complexity of $O(N)$ and a space complexity of $O(N)$.

5.2.2 Routing Discovery Phase

Traditional ant colony-based routing suffers from the local optimum problem and energy imbalance due to its reliance on a single heuristic factor. Our solution tackles this issue by refining the node transition probability formula $P(k)$ to incorporate a multi-dimensional heuristic. By integrating factors for node energy, distance, and angle into the route discovery process, the algorithm achieves intelligent, load-balanced next-hop selection, leading to more energy-efficient and globally optimal paths. The routing discovery process iterates through all candidate nodes in the allowable set. For each candidate node, the distance factor, directional factor cos(θ), and energy factor are calculated. Candidates with insufficient energy are excluded from the candidate set. Then, the distance, directional, and energy factors are normalized within the current candidate set before calculating the node transition probability P(k). This normalization prevents any single factor from dominating the heuristic function due to inconsistent numerical scales. The next hop is then selected through the roulette wheel method. The detailed procedure is described in Algorithm 3. To be specific, the specific description is described by the pseudo-code as shown in Algorithm 3.

Algorithm 3: Routing discovery pseudocode

INPUT: Allow: the set of candidate nodes after pre-screening; Table: ant path information table; m_i: current ant index; n_i: current path-position index
OUTPUT: Get the routing path information after an iteration is completed
1: **for** k ← 1: length(Allow) **do**
2: Calculate the distance factor, directional factor cos (θ_{sij}), and energy factor EF for Allow(k)
3: Exclude Allow(k) from the candidate set if EF ≤ 0
4: **end for**
5: Normalize the distance, directional, and energy factors within the current candidate set
6: for k ← 1: length(Allow) **do**
7: Calculate the transfer probability of node Allow(k) based on the improved node transfer probability formula: P(k)
8: **end for**

(Continued)

Algorithm 3 (continued)

9: Determine the next hop of the route according to the roulette method: Target
10: Add the next-hop node to the path information table: $Table\,(m_i, n_i) = Target$
11: **if** the next hop is the target node **do**
12: Return the current routing path and terminate the current route discovery process
13: **end if**

In terms of time complexity, Algorithm 3 needs to traverse the candidate node set and calculate the angle factor, energy factor, and transition probability for each candidate. In the worst-case scenario, the candidate node set includes all network nodes, with a scale of $O(N)$, so the loop's time complexity is $O(N)$. The roulette wheel selection mechanism requires constructing a cumulative probability distribution and performing random selection, with a time complexity also of $O(N)$. In terms of space complexity, the algorithm needs to store data, with a total space requirement of $O(N)$. Additionally, the algorithm must maintain routing path information, with a space complexity of $O(N)$. Overall, Algorithm 3 has a time complexity of $O(N)$ and a space complexity of $O(N)$.

5.2.3 Pheromone Update Phase

The pheromone update phase consists of two stages, namely the pheromone increase stage and the pheromone volatilization stage. The former adopts the path-pheromone accumulation method in the traditional ant colony algorithm, and the latter adopts the pheromone dynamic replenishment mechanism for the secondary pheromone update. In this paper, a pheromone dynamic replenishment mechanism is proposed to avoid suboptimal routes. It enhances the standard two-stage process, namely comprising pheromone augmentation and volatilization, by incorporating an adaptive replenishment step. The mechanism first performs path-specific pheromone reinforcement based on route quality. It then applies controlled global evaporation to prevent stagnation. Crucially, a dynamic replenishment operation is triggered when pheromone levels on any edge drop below a minimum threshold $T_{\min}$, reintroducing a moderated amount of pheromone to sustain path diversity. This process not only preserves the positive feedback inherent in the original ant colony optimization but also prevents the route exploration from becoming trapped in local optima by augmenting it with a dynamic replenishment mechanism. Specifically, the details are described by the pseudo-code in Algorithm 4.

Algorithm 4: Pheromone update pseudocode

INPUT: Tau: Path pheromone matrix; Table: Ant path information table; Length: Routing path length; Ptau: Pheromone increment; Rho1, Rho2: Pheromone evaporation rates; Rho3: Pheromone replenishment rate; Tmin: Minimum pheromone threshold; Min, Max: Bounds of replenishment times
OUTPUT: Perform updates of pheromones on the path
1: **for** m_i ← 1 to M **do**
2: **for** n_i ← 2 to N **do**
3: $i = Table\,(m_i, n_{i-1}),\quad j = Table\,(m_i, n_i)$
4: **if** edge (i, j) belongs to the routing path of ant mi **do**
5: Tau(i, j) = (1-Rho1) × Tau(i, j) + Ptau(i, j)
6: **end if**
7: **end for**
8: **end for**
9: **for** i ← 1 to N **do**

(Continued)

Algorithm 4 (continued)

```
    for j ← 1 to N do
        if Ptau(i, j) = 0 do
            Tau(i, j) = (1-Rho2) × Tau(i, j)
        end if
        if Tau(i, j) < T_min do
            ri = randi(Min, Max)
            Tau(i, j) = (1 + Rho3)^ri × Tau(i, j)
        end if
    end for
end for
```

5.3 Time Complexity Analysis

For Algorithm 4, in terms of time complexity, the first phase of path pheromone enhancement traverses the path information of all ants. The outer loop iterates through M ants, while the inner loop traverses the path nodes, with a maximum path length of N, resulting in a time complexity of $O(M \cdot N)$. The second phase of global pheromone evaporation traverses all $N \times N$ elements of the pheromone matrix, with a time complexity of $\mathrm{O}\left(N^2\right)$. In terms of space complexity, the algorithm primarily relies on the pheromone matrix, which has a size of $N \times N$, resulting in a space complexity of $\mathrm{O}(N^2)$. Additionally, the algorithm needs to store path length information and temporary computation variables, but the auxiliary space requirement for these is $O(M \cdot N)$. Taking all factors into consideration, Algorithm 4 has a time complexity of $\mathrm{O}(N^2 + M \cdot N)$ and a space complexity of $\mathrm{O}\left(N^2\right)$.

To evaluate the practical feasibility of ELRAC in resource-constrained wireless sensor networks, this section provides a theoretical analysis of its computational efficiency from both time and space complexity perspectives.

The main algorithm consists of T rounds of iterations, each requiring three operations: neighbor pre-screening, route discovery, and pheromone update. In the pre-screening phase, Algorithm 2 has a time complexity of $\mathrm{O}(N)$ for each execution. Since Algorithm 1 invokes Algorithm 2 inside the inner loop over n_i for each of the M ants, the pre-screening cost in each round is $\mathrm{O}(M \cdot N^2)$. During route discovery, under the worst-case scenario where the candidate set size is N, each ant requires N transfer probability calculations and roulette wheel selections, leading to a per-round time complexity of $\mathrm{O}(M \cdot N^2)$. The pheromone update operation involves traversing all edges, with a complexity of $\mathrm{O}(N^2)$. Since the $M \cdot N^2$ term is typically dominant, the overall time complexity can be expressed as $\mathrm{O}(T \cdot M \cdot N^2)$.

Regarding space complexity, the algorithm maintains four primary data structures in memory: an $M \times N$ table storing ant path information, an $N \times N$ symmetric matrix recording inter-node distances, an $N \times N$ matrix preserving edge pheromone concentrations, and auxiliary vectors for energy, angle, and hierarchy parameters, each of length N. This configuration results in a total space complexity of $\mathrm{O}(N^2 + M \cdot N)$.

6 Experiments and Results Analysis

In this section, the superiority of our proposal is validated through extensive simulations across three key metrics: (1) network lifetime, (2) throughput, and (3) energy consumption. Three network scenarios are considered: (a) n = 600 with a topology range of 250 m × 250 m × 10 m, (b) n = 800 with a topology range

of 300 m × 300 m × 10 m, and (c) n = 1000 with a topology range of 350 m × 350 m × 10 m. The statistical validation, ablation study, and parameter sensitivity analysis are conducted under the 800-node scenario.

6.1 Experiment and Parameters Settings

The simulation was conducted based an AMD Ryzen™ 9 5900HX CPU @ 3.30 GHz. Java 8 was employed as the programming language for the experiments. The initial energy of each node was set to 0.5 J, and the minimum energy threshold was defined as 0.05 J. The size of each data packet was configured to 3000 bits. εfs was 10 pJ/bit/m^2, εmp was 0.0013 pJ/bit/m^4, and E_{elec} was 50 nJ/bit. The energy consumption for data aggregation was assumed to be 5 nJ/bit.

For convenience, all parameters used in the simulation are summarized in Table 2.

Table 2: Simulation parameters.

Parameters	Values
Network size	250 m × 250 m × 10 m 300 m × 300 m × 10 m 350 m × 350 m × 10 m
Size of package l Initial energy of nodes	3000 bits 0.5 J
Energy consumed per bit to send or receive E_{elec}	50 nJ/bit
Energy consumption of free space amplifier εfs	10 pJ/bit/m^2
Energy consumption of multipath amplifier ε_{mp}	0.0013 pJ/bit/m^4
Energy consumption of aggregation E_{da}	5 nJ/bit
Distance threshold for information transmission d_0	87

6.2 Results Analysis

6.2.1 Evaluation in Network Lifetime

In this section, the network lifetime, which is defined by the time of the First Node Dead (FND), that of Half of Node Dead (HND) and that of All Node Dead (AND), is adopted as a main metric to compare the performance between our proposal and other protocols.

Fig. 7 illustrates the relationship between the number of rounds and the number of dead nodes for different protocols. In addition, Fig. 8 compares the FND, HND, and AND of each protocol. It can be observed that ELRAC maintains a relatively smooth increase in the number of dead nodes during the main working period of the network. Compared with LEACH, ELRAC avoids the rapid collapse after the first node death and maintains a much longer effective operation period. Compared with GWOA-CH, ELRAC obtains better FND and HND in the repeated simulations, although its AND is close to that of GWOA-CH rather than absolutely dominant. This indicates that ELRAC is more effective in maintaining useful network operation instead of only delaying the death of the last few residual nodes.

The improvement of ELRAC in network lifetime is mainly attributed to the joint effect of the energy factor and the angle factor. The energy factor prevents low-energy nodes from being repeatedly selected as forwarding nodes, while the angle factor reduces detoured forwarding and guides packets toward the Sink. Therefore, ELRAC can alleviate local energy holes and achieve a more balanced energy consumption process. Although R-LEACH may show a better HND in some scenarios due to residual-energy-based cluster-head rotation, its data delivery performance is lower than that of ELRAC. Thus, ELRAC achieves a better trade-off between network lifetime and effective data transmission.

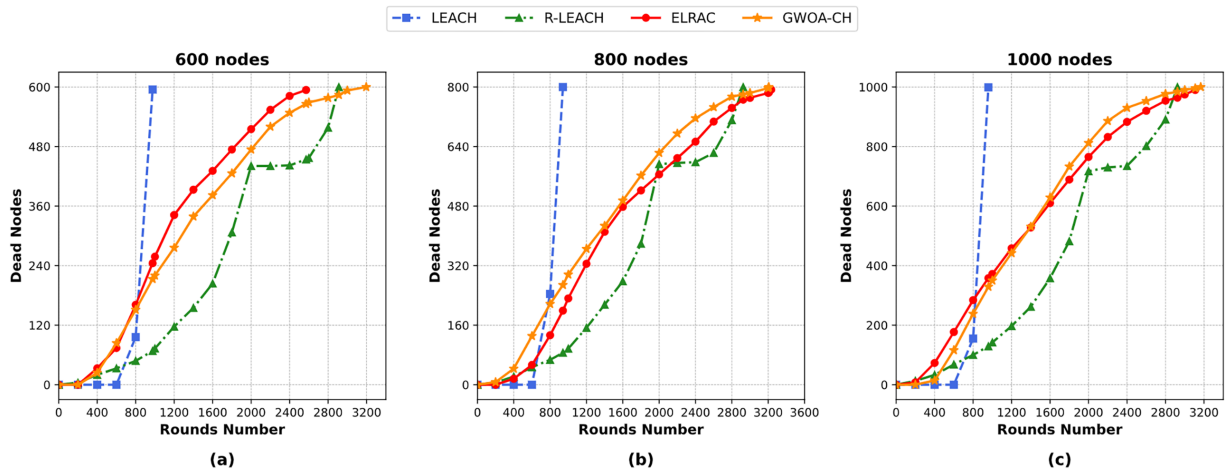


Figure 7: Comparisons on the number of dead nodes. (**a**) n = 600, 250 m × 250 m × 10 m; (**b**) n = 800, 300 m × 300 m × 10 m; (**c**) n = 1000, 350 m × 350 m × 10 m.

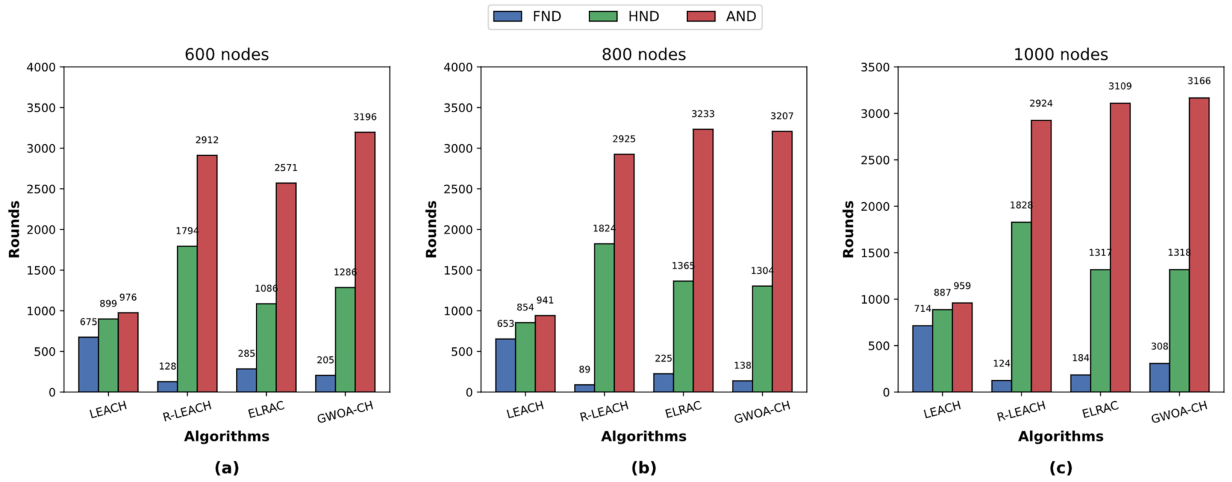


Figure 8: Comparisons on the network lifetime in terms of FND, HND, and AND. (**a**) n = 600, 250 m × 250 m × 10 m; (**b**) n = 800, 300 m × 300 m × 10 m; (**c**) n = 1000, 350 m × 350 m × 10 m.

6.2.2 Evaluation in Throughput

In this paper, the throughput is defined as the amount of data received by the Sink in each round. The performance comparisons among different protocols are presented in the following three metrics: (1) packets received by the Sink, refers to the total amount of data received by the Sink from the beginning of network operation until the i-th round; (2) the network throughput, indicates the amount of data received by the sink node during the single round of the *i*-th round; and (3) the average network throughput, represents the average per-round transmission performance from the 1st round to the *i*-th round.

Fig. 9 illustrates the total number of packets received by the Sink. It can be readily observed that ELRAC achieves the best packet delivery performance among the compared protocols under all tested network scales. Compared with LEACH and R-LEACH, ELRAC delivers substantially more packets to the Sink, and it also maintains a clear advantage over GWOA-CH. This indicates that ELRAC can keep more effective forwarding paths during network operation and improve the overall data collection capacity. This is mainly because the Energy Factor (EF), Angle Factor, and pheromone information jointly guide route selection, while the

neighbor pre-screening mechanism reduces ineffective forwarding candidates. Consequently, more packets can be delivered to the Sink under the same network configuration.

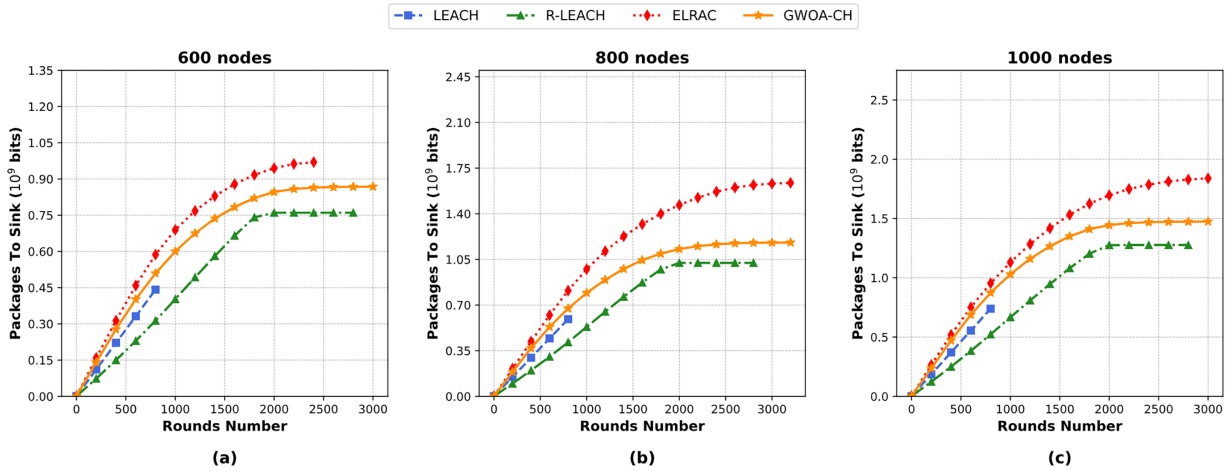


Figure 9: Comparisons on the number of packets received by the Sink. (**a**) n = 600, 250 m × 250 m × 10 m; (**b**) n = 800, 300 m × 300 m × 10 m; (**c**) n = 1000, 350 m × 350 m × 10 m.

Fig. 10 illustrates the per-round throughput of different protocols. The throughput of LEACH and R-LEACH declines rapidly after a short stable period, while GWOA-CH remains relatively stable before gradually decreasing. In contrast, ELRAC starts with the highest initial throughput and then decreases over time. This is because ELRAC activates more forwarding nodes and establishes more effective routes in the early stage, which improves data collection but also causes faster energy consumption. As dead nodes increase, the number of available forwarding nodes decreases, and the throughput curves of all protocols gradually decline. Nevertheless, ELRAC still maintains a higher throughput than the benchmark protocols during most of the effective working period.

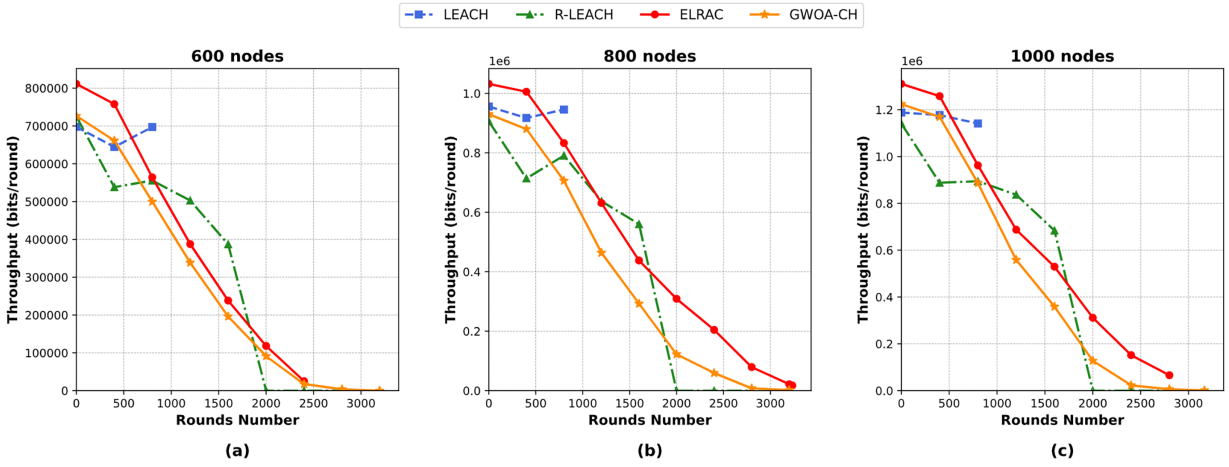


Figure 10: Comparisons on the throughput per round. (**a**) n = 600, 250 m × 250 m × 10 m; (**b**) n = 800, 300 m × 300 m × 10 m; (**c**) n = 1000, 350 m × 350 m × 10 m.

Fig. 11 illustrates the average throughput of different protocols. It can be seen that ELRAC achieves the highest average throughput in most rounds, followed by GWOA-CH, R-LEACH, and LEACH. Although the

high-throughput advantage of ELRAC gradually weakens in the later stage, its average throughput remains at a relatively high level for a longer period. This result further confirms that the proposed routing strategy can improve not only the instantaneous throughput, but also the long-term data collection performance of the network. Moreover, the dynamic pheromone update mechanism helps adjust forwarding paths when some nodes consume energy rapidly, thereby avoiding long-term dependence on a few high-quality nodes.

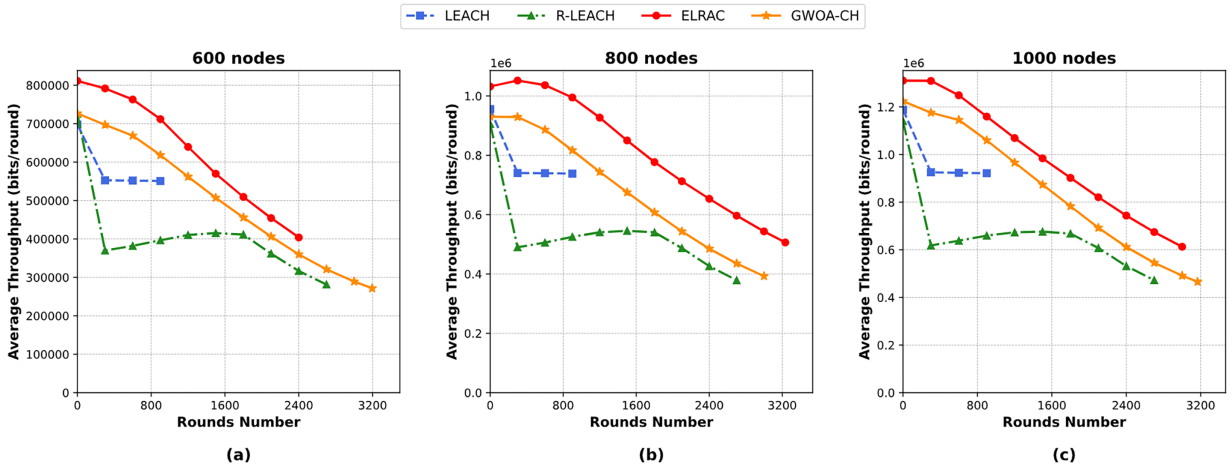


Figure 11: Comparisons on the average throughput. (**a**) n = 600, 250 m × 250 m × 10 m; (**b**) n = 800, 300 m × 300 m × 10 m; (**c**) n = 1000, 350 m × 350 m × 10 m.

6.2.3 Energy Consumption

Fig. 12 presents the percentage of total energy consumed by different protocols. Experimental results indicate that the energy consumption of all protocols increases with the progression of rounds, while the growth rate gradually slows down after more nodes become dead. This is because the number of active nodes decreases in the later stage, reducing the amount of sensing, receiving, and forwarding operations.

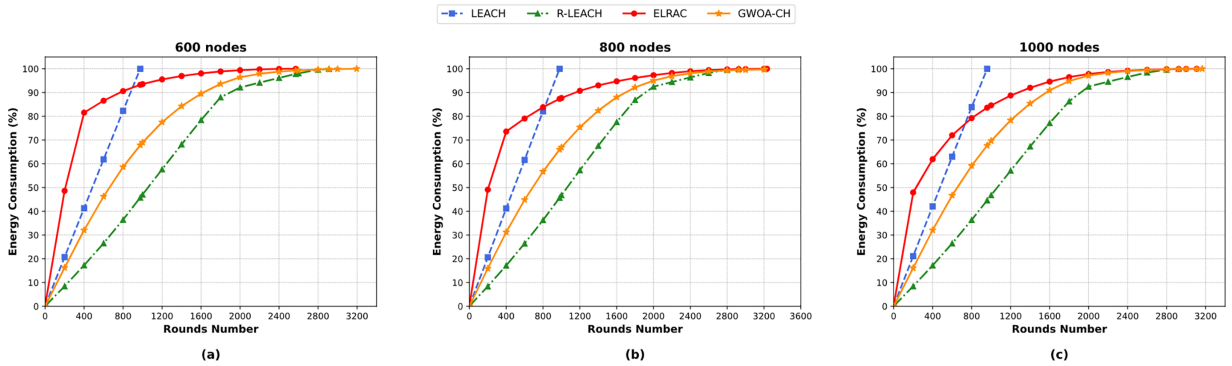


Figure 12: Comparisons on total energy consumption. (**a**) n = 600, 250 m × 250 m × 10 m; (**b**) n = 800, 300 m × 300 m × 10 m; (**c**) n = 1000, 350 m × 350 m × 10 m.

It can be observed that ELRAC consumes energy faster in the early stage than the other protocols. This phenomenon is directly related to its higher throughput. Since ELRAC establishes more effective forwarding paths and allows more nodes to participate in data transmission, more energy is consumed during the main data collection period. However, this energy consumption is not ineffective consumption; it is converted into

a larger amount of data received by the Sink. Therefore, the early energy consumption of ELRAC should be interpreted together with its packet delivery performance.

Fig. 13 illustrates the average energy consumption per round. The average energy consumption of ELRAC is relatively high at the beginning and then decreases gradually as the network degrades. Compared with protocols that consume less energy but deliver fewer packets, ELRAC shows a more active data collection strategy. This result also explains why ELRAC can achieve higher throughput and energy efficiency despite its higher early-stage energy consumption.

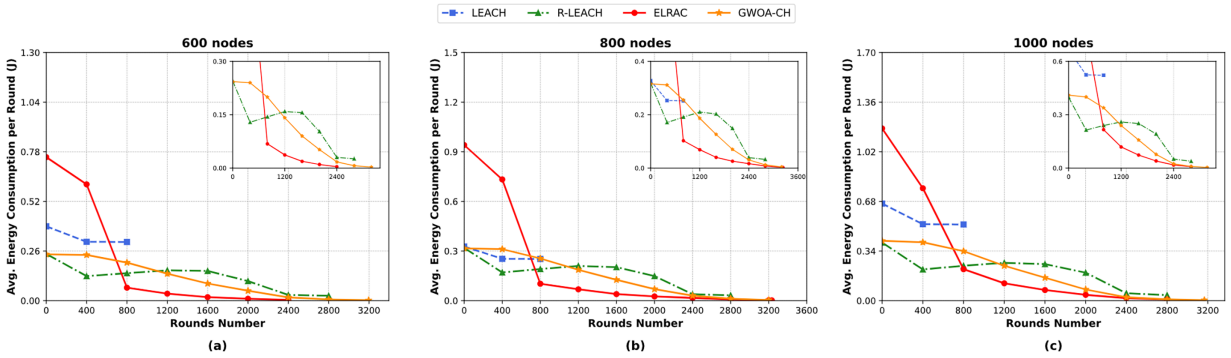


Figure 13: Comparisons on energy consumption per round. (**a**) n = 600, 250 m × 250 m × 10 m; (**b**) n = 800, 300 m × 300 m × 10 m; (**c**) n = 1000, 350 m × 350 m × 10 m.

6.2.4 Energy Efficiency

In this paper, energy efficiency is defined as the ratio of the number of packets received by the Sink to the energy consumption of sensor nodes.

Fig. 14 presents the energy efficiency of our proposal and the benchmarks. It can be observed that ELRAC is lower than GWOA-CH and R-LEACH at the early stage in some scenarios. This is mainly because ELRAC consumes more energy at the beginning by activating more forwarding nodes and transmitting more packets to the Sink. Therefore, its early-stage energy efficiency is temporarily affected by the rapid energy consumption. However, as the network continues to operate, ELRAC gradually achieves the highest energy efficiency among the compared protocols. Although ELRAC consumes more energy in the early stage, it also delivers a larger amount of data to the Sink during the effective working period. Therefore, the early energy consumption is effectively converted into useful data transmission rather than being wasted on ineffective forwarding.

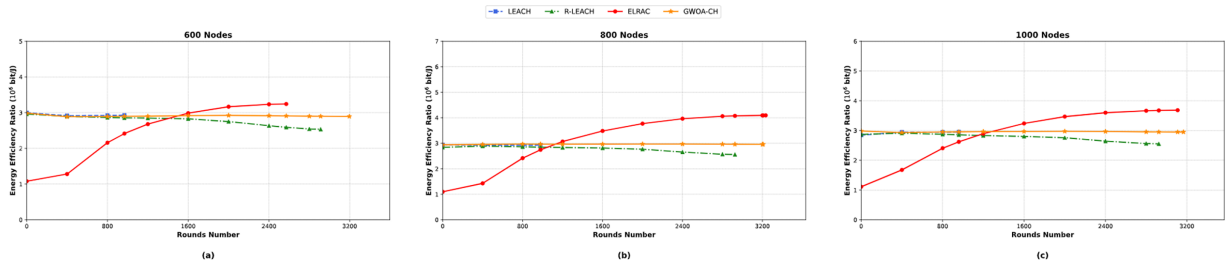


Figure 14: Comparisons on the energy efficiency of different protocols. (**a**) n = 600, 250 m × 250 m × 10 m; (**b**) n = 800, 300 m × 300 m × 10 m; (**c**) n = 1000, 350 m × 350 m × 10 m.

The higher energy efficiency of ELRAC benefits from the joint effect of neighbor pre-screening, energy-aware routing, angle-based guidance, and pheromone update. These mechanisms reduce ineffective forwarding, avoid excessive use of low-energy nodes, and maintain route diversity. Consequently, ELRAC can achieve better data delivery under the same energy budget, leading to a higher overall energy efficiency than the benchmark protocols.

6.2.5 Statistical Validation and Comparison with Recent State-of-the-Art Method

To further verify the stability of the experimental results, each protocol was independently simulated ten times under the 800-node scenario. The same set of random topology files was used for all compared protocols to ensure fairness. The mean and standard deviation of the main metrics are reported in Table 3.

Table 3: Statistical comparison with recent state-of-the-art methods under the 800-node scenario.

Algorithm	FND (Rounds)	HND (Rounds)	AND (Rounds)	Packets to Sink (10^9 bits)	Energy Efficiency (10^6 bit/J)
LEACH	660.0 ± 67.1	907.1 ± 36.2	982.5 ± 28.1	0.726 ± 0.021	2.947 ± 0.019
R-LEACH	125.1 ± 27.1	1793.0 ± 32.8	2901.7 ± 20.1	1.018 ± 0.014	2.545 ± 0.036
GWOA-CH	179.0 ± 30.9	1298.1 ± 15.8	3422.0 ± 170.4	1.164 ± 0.009	2.916 ± 0.023
AEGWO-CH	122.9 ± 16.8	1340.6 ± 14.2	3389.9 ± 157.0	1.143 ± 0.012	2.865 ± 0.031
ELRAC	218.6 ± 23.3	1428.0 ± 40.7	3393.2 ± 94.6	1.687 ± 0.034	4.217 ± 0.084

Table 3 reports the mean and standard deviation of FND, HND, AND, packets received by the Sink, and energy efficiency. In addition to LEACH, R-LEACH, and GWOA-CH, Adaptive Enhanced Grey Wolf Optimizer-based cluster-head selection (AEGWO-CH) is included in the table as a recent GWO-based clustering protocol. Since the time-series curves of AEGWO-CH and GWOA-CH are close under the same simulation configuration, AEGWO-CH is reported in the statistical table rather than being repeated in every line figure, so that the readability of the main figures can be maintained.

As shown in Table 3, ELRAC achieves the highest packet delivery and energy efficiency among all compared algorithms. Compared with GWOA-CH, AEGWO-CH, R-LEACH, and LEACH, ELRAC achieves consistently higher packet delivery to the Sink under the same 800-node scenario. This result demonstrates that the proposed routing strategy can maintain stronger data-collection capability while making more effective use of the available energy resources. In terms of energy efficiency, ELRAC also achieves the best result because it delivers more useful data under the same initial energy budget. For network lifetime, ELRAC obtains higher FND and HND than both GWOA-CH and AEGWO-CH, while its AND is slightly lower than that of the two GWO-based methods. This result indicates that ELRAC focuses on improving effective data collection and balanced network operation rather than merely extending the death time of the last remaining nodes.

To further quantify the stability of the simulation results, 95% confidence intervals were calculated for the ten independent runs. The confidence interval was computed as mean ± 1.96 sigma/sqrt(n), where n = 10. Table 4 lists the confidence intervals of the compared algorithms.

Table 4: 95% Confidence intervals over ten random topologies.

Algorithm	FND	HND	AND	Packets to Sink (10^9 bits)	Energy Efficiency (10^6 bit/J)
LEACH	660.0 [618.4, 701.6]	907.1 [884.7, 929.5]	982.5 [965.1, 999.9]	0.726 [0.713, 0.738]	2.947 [2.934, 2.959]
R-LEACH	125.1 [108.3, 141.9]	1793.0 [1772.6, 1813.4]	2901.7 [2889.2, 2914.2]	1.018 [1.009, 1.027]	2.545 [2.523, 2.567]
GWOA-CH	179.0 [159.9, 198.1]	1298.1 [1288.3, 1307.9]	3422.0 [3316.4, 3527.6]	1.164 [1.159, 1.169]	2.916 [2.902, 2.930]
AEGWO-CH	122.9 [112.5, 133.3]	1340.6 [1331.8, 1349.4]	3389.9 [3292.6, 3487.2]	1.143 [1.135, 1.150]	2.865 [2.845, 2.884]
ELRAC	218.6 [204.2, 233.0]	1428.0 [1402.8, 1453.2]	3393.2 [3334.5, 3451.9]	1.687 [1.666, 1.708]	4.217 [4.164, 4.269]

The confidence intervals show that the packet-delivery and energy-efficiency advantages of ELRAC are stable across different random topologies. Although the AND of ELRAC is close to that of GWOA-CH and AEGWO-CH, the intervals of packets received by the Sink and energy efficiency are clearly separated from those of the benchmark protocols.

Two-sided Welch t-tests were further conducted between ELRAC and each baseline protocol. Table 5 reports the corresponding p-values. The results show that ELRAC achieves statistically significant improvements in packet delivery and energy efficiency over all compared protocols. The AND difference between ELRAC and GWOA-CH or AEGWO-CH is not statistically significant, which is consistent with the observation that the proposed method emphasizes effective data collection during the useful network lifetime.

Table 5: Welch t-test p-values between ELRAC and baselines.

Baseline vs. ELRAC	FND	HND	AND	Packets to Sink	Energy Efficiency
GWOA-CH vs. ELRAC	4.89×10^{-3}	8.68×10^{-7}	0.648	2.44×10^{-13}	2.19×10^{-13}
AEGWO-CH vs. ELRAC	1.03×10^{-8}	4.68×10^{-5}	0.955	1.58×10^{-14}	1.66×10^{-14}
R-LEACH vs. ELRAC	1.80×10^{-7}	4.48×10^{-14}	2.27×10^{-8}	3.48×10^{-16}	3.55×10^{-16}
LEACH vs. ELRAC	5.36×10^{-10}	1.00×10^{-16}	6.67×10^{-16}	8.72×10^{-21}	5.70×10^{-13}

6.2.6 Ablation Study

To further verify the effectiveness of the key components in ELRAC, an ablation study was conducted under the 800-node scenario. Four variants were constructed by removing one component at a time: the angle factor, the energy factor, the neighbor pre-screening mechanism, and the dynamic pheromone replenishment mechanism. All variants used the same network configuration and simulation settings as the complete ELRAC protocol, so that the performance variation could be attributed to the removed component.

Table 6 summarizes the network lifetime and packet delivery performance of the complete ELRAC and its ablation variants. The complete ELRAC achieves a balanced overall performance. Removing the energy factor causes the most severe degradation. The FND decreases from 236 to 13 rounds, the HND decreases from 1374 to 341 rounds, and the total packets received by the Sink decrease by 74.4%. This indicates that the energy factor is critical for avoiding overloaded forwarding nodes and preventing the formation of energy holes.

The angle factor also contributes positively to the routing process. Without the angle factor, FND, HND, AND, and packet delivery all decrease, demonstrating that directional guidance helps avoid detoured or backward forwarding and improves routing efficiency. Removing the dynamic pheromone replenishment

mechanism leads to a moderate reduction in HND, AND, and packet delivery, suggesting that this mechanism mainly improves long-term route diversity and route maintenance stability rather than dominating every single routing decision.

Table 6: Ablation study of ELRAC under the 800-node scenario.

Algorithm	Removed Component	FND	HND	AND	Packets to Sink	Packet Change
ELRAC	None	236	1374	3251	1,641,602,400	–
w/o Angle	Angle factor	188	1182	3072	1,340,979,000	−18.3%
w/o Energy	Energy factor	13	341	1128	420,198,000	−74.4%
w/o Pre-screening	Neighbor pre-screening	265	1458	3145	1,651,153,800	+0.6%
w/o Replenishment	Pheromone replenishment	239	1287	3059	1,525,044,000	−7.1%

Note: Packet change is calculated relative to the complete ELRAC. Positive values in a single run do not necessarily indicate overall superiority; they should be interpreted together with lifetime, routing overhead, and repeated-run statistics when available.

The neighbor pre-screening mechanism shows a different effect. Removing it does not always reduce FND or HND in a single run, because a larger candidate set may occasionally provide more forwarding choices. However, this comes at a much higher routing-search cost. Therefore, the contribution of the pre-screening mechanism should be evaluated mainly from routing overhead and computational efficiency rather than only from lifetime metrics.

Table 7 further verifies the role of the neighbor pre-screening mechanism. After the pre-screening mechanism is removed, the average candidate size increases from 164.89 to 418.81, corresponding to approximately 2.54 times the search space. The average candidate evaluations and estimated control-message exchanges per round also increase by about 2.49 times, while the runtime per round increases by about 2.62 times. These results demonstrate that the neighbor pre-screening mechanism effectively reduces route discovery overhead and improves computational efficiency.

Table 7: Routing-overhead comparison with and without neighbor pre-screening.

Metric	ELRAC	w/o Pre-Screening	Relative Increase
Avg. candidate size	164.89	418.81	2.54×
Avg. candidate evaluations per round	158,501	395,411	2.49×
Avg. estimated control-message exchanges per round	317,002	790,821	2.49×
Runtime per round	109.55 ms	287.42 ms	2.62×

Overall, the ablation results confirm that the proposed components contribute to ELRAC from different perspectives. The energy factor provides the strongest contribution to network lifetime and packet delivery, the angle factor improves directional routing efficiency, the pheromone replenishment mechanism enhances long-term route maintenance, and the neighbor pre-screening mechanism substantially reduces routing overhead. The complete ELRAC therefore achieves a more balanced trade-off among network lifetime, throughput, route diversity, and computational cost.

6.2.7 Parameter Sensitivity Analysis

To evaluate the influence of key parameters on ELRAC, a parameter sensitivity analysis was conducted under the same 800-node simulation setting, as summarized in Table 8. In each group of experiments, only one parameter is varied while the remaining parameters are fixed at their default values. The selected value is determined according to the overall trade-off among network lifetime, packets received by the Sink, energy efficiency, and routing stability.

Table 8: Parameter sensitivity analysis of ELRAC.

Parameter	Tested Values	Selected Value	Observation
alpha	1.0, 1.5, 2.0	1.0	A larger alpha increases the influence of distance-related routing preference; the selected value should balance short paths and load distribution.
beta	0.5, 1.0, 1.5	0.5	Controls the contribution of angle-based directional guidance; an appropriate value helps avoid detoured or backward forwarding.
gamma	1.0, 2.0, 3.0	2.0	Controls the contribution of residual-energy awareness; a moderate value helps avoid energy holes without over-concentrating traffic.
rho	0.01, 0.03, 0.05	0.03	Represents the pheromone evaporation rate; too small a value may slow adaptation, whereas too large a value may weaken route memory.
$T_{\min}$	0.001, 0.01, 0.05	0.01	Lower bound of pheromone intensity; it prevents pheromone disappearance and maintains basic exploration capability.
Number of ants	30, 50, 100	100	More ants increase route exploration but also increase computational cost; the selected value should balance performance and runtime.

6.2.8 Computational Overhead Analysis

In addition to packet delivery and energy efficiency, the computational overhead of each algorithm was evaluated by recording the actual runtime under the same simulation environment. Since different protocols have different network lifetimes and routing procedures, runtime per round was adopted as a unified metric for comparison. As shown in Table 9, LEACH and R-LEACH require the lowest runtime because they rely on relatively simple clustering and forwarding rules. GWOA-CH and AEGWO-CH introduce swarm-intelligence-based optimization, and therefore require higher computational cost.

As shown in Table 9, LEACH and R-LEACH require the lowest runtime because they rely on relatively simple clustering and forwarding rules. GWOA-CH and AEGWO-CH introduce swarm-intelligence-based optimization, and therefore require higher computational cost. ELRAC has the highest runtime among the compared protocols, mainly because it performs multi-factor route evaluation by jointly considering distance, forwarding angle, residual energy, neighbor pre-screening, and dynamic pheromone updating. These operations increase the computational burden during route discovery and route maintenance.

More importantly, the additional computational cost is accompanied by higher packet delivery and energy efficiency, as demonstrated in the previous sections. Therefore, ELRAC achieves a reasonable trade-off between computational overhead and network performance.

Table 9: Runtime comparison of different algorithms.

Algorithm	Runtime Per Run	Runtime Per Round	Relative Runtime	Remark
LEACH	274.98 ms	0.2820 ms	1.00×	Classical clustering baseline
R-LEACH	532.66 ms	0.1817 ms	0.64×	Residual-energy-based clustering
GWOA-CH	5051.17 ms	1.6122 ms	5.72×	GWO-based clustering baseline
AEGWO-CH	88283.31 ms	26.1891 ms	92.86×	Recent GWO-based baseline
ELRAC	170089.03 ms	49.8795 ms	176.85×	Proposed multi-factor ACO routing

7 Conclusions and Future Works

In this paper, an energy-efficient and load-balanced routing protocol, named ELRAC, is proposed for wireless sensor networks. ELRAC integrates a hierarchical network model, an angle-based neighbor pre-screening mechanism, a composite heuristic function, and a dynamic pheromone replenishment strategy. The neighbor pre-screening mechanism reduces ineffective candidate interactions during route discovery, while the composite heuristic function jointly considers distance, direction, and residual energy to guide packets toward energy-efficient and load-balanced forwarding paths. In addition, the dynamic pheromone replenishment mechanism helps maintain route diversity and alleviates premature convergence. Simulation results demonstrate that ELRAC achieves better overall performance than the compared protocols in terms of network lifetime, packet delivery, throughput, and energy efficiency.

In future work, we will further improve the computational efficiency of ELRAC and evaluate its scalability in larger and denser WSN scenarios. We will also investigate adaptive parameter tuning strategies to reduce manual parameter selection and improve the adaptability of the protocol. Moreover, integrating simultaneous wireless information and power transfer (SWIPT) and UAV-assisted sensing/data collection will be explored to enhance the sustainability and applicability of ELRAC in mobile and dynamic next-generation IoT scenarios.

Acknowledgement: Not applicable.

Funding Statement: This work is supported by the National Natural Science Foundation of China under Grant No. 62461041, Natural Science Foundation of Jiangxi Province under Grant No. 20242BAB25068, and China Scholarship Council under Grant No. 202106825021.

Author Contributions: Kexin Liao: Writing and Investigation; Deyu Lin: Conceptualization and Theory analysis; Ran Hu: Writing and Revising; Yufei Zhao: Writing and Original draft preparation; Yong Liang Guan: Writing and Investigation. All authors reviewed and approved the final version of the manuscript.

Availability of Data and Materials: Some or all data, models, or code generated or used during the study are available from the corresponding author by request.

Ethics Approval: Ethical approval was not required for this study. This work focuses on the algorithm simulation and performance analysis of wireless sensor networks, without involving human participants, animal experiments or private sensitive data collection.

Conflicts of Interest: The authors declare no conflicts of interest.

References

1. Al-Fuqaha A, Guizani M, Mohammadi M, Aledhari M, Ayyash M. Internet of Things: a survey on enabling technologies, protocols, and applications. IEEE Commun Surv Tutor. 2015;17(4):2347–76. doi:10.1109/comst.2015.2444095.
2. Lin J, Yu W, Zhang N, Yang X, Zhang H, Zhao W. A survey on Internet of Things: architecture, enabling technologies, security and privacy, and applications. IEEE Internet Things J. 2017;4(5):1125–42. doi:10.1109/JIOT.2017.2683200.
3. Vlachos M, Papathanasiou C, Tsiakos V, Tsimiklis G, Amditis A. Low-cost sensing solutions for harsh environments: exploring wireless and satellite solutions in desert environmental monitoring. In: Proceedings of the IGARSS 2024–2024 IEEE International Geoscience and Remote Sensing Symposium; 2024 Jul 7–12; Athens, Greece. New York, NY, USA: IEEE; 2024. p. 7525–8. doi:10.1109/IGARSS53475.2024.10642661.
4. Koo YC, Mahyuddin MN, Wahab MNA. Novel control theoretic consensus-based time synchronization algorithm for WSN in industrial applications: convergence analysis and performance characterization. IEEE Sens J. 2023;23(4):4159–75. doi:10.1109/JSEN.2022.3231726.
5. Jeyakarthic M, Suganya R, Kavitha K. Develop an advanced UAV-WSN system for intelligent precision agriculture monitoring. In: Proceedings of the 2025 7th International Conference on Signal Processing, Computing and Control (ISPCC); 2025 Mar 6–8; Solan, India. New York, NY, USA: IEEE; 2025. p. 997–1002. doi:10.1109/ISPCC66872.2025.11039394.
6. Yao YD, Li X, Cui YP, Wang JJ, Wang C. Energy-efficient routing protocol based on multi-threshold segmentation in wireless sensors networks for precision agriculture. IEEE Sens J. 2022;22(7):6216–31. doi:10.1109/JSEN.2022.3150770.
7. Sonai V, Bharathi I. A new statistical compression-based method for wireless sensor networks energy efficient data transmission. IEEE Sens Lett. 2024;8(3):6002804. doi:10.1109/LSENS.2024.3367044.
8. Anand S, Rachitha HN. Enhancing energy efficiency routing protocol for wireless sensor network using ACO algorithm. In: Proceedings of the 2022 IEEE North Karnataka Subsection Flagship International Conference (NKCon); 2022 Nov 20–21; Vijaypur, India. New York, NY, USA: IEEE; 2023. p. 1–5. doi:10.1109/NKCon56289.2022.10126842.
9. Xia S, Wu S, Ni J. A new energy-efficient routing algorithm based on ant colony system for wireless sensor networks. In: Proceedings of the 2009 Fourth International Conference on Internet Computing for Science and Engineering; 2009 Dec 21–22; Harbin, China. New York, NY, USA: IEEE; 2010. p. 176–80. doi:10.1109/ICICSE.2009.27.
10. Liu J, Zhang H. Height-fixed UAV enabled energy-efficient data collection in RIS-aided wireless sensor networks. IEEE Trans Wirel Commun. 2023;22(11):7452–63. doi:10.1109/twc.2023.3250988.
11. Huang H, Zhang J, Wang B, Miao W, Min G. Joint mobile energy replenishment and data gathering in wireless sensor networks via federated deep reinforcement learning. IEEE Trans Mob Comput. 2025;24(7):6460–73. doi:10.1109/TMC.2025.3543009.
12. Zhu T, Li J, Gao H, Li Y, Cai Z. AoI minimization data collection scheduling for battery-free wireless sensor networks. IEEE Trans Mob Comput. 2021;22(3):1343–55. doi:10.1109/tmc.2021.3106013.
13. Tian Y, Wang L, Lin C, Han B, Zhang L, Zhou Z, et al. Zero-knowledge neighbor discovery for underwater optical wireless sensor networks. IEEE Trans Mob Comput. 2025;24(11):11596–613. doi:10.1109/tmc.2025.3581371.
14. Zhang T, Gou Y, Liu J, Cui JH. Traffic load-aware resource management strategy for underwater wireless sensor networks. IEEE Trans Mob Comput. 2025;24(1):243–60. doi:10.1109/tmc.2024.3459896.
15. Wang C, Liu G, Jiang T. Malicious node detection in wireless weak-link sensor networks using dynamic trust management. IEEE Trans Mob Comput. 2024;23(12):12866–77. doi:10.1109/tmc.2024.3418826.
16. Xiao Z, Liu S, Lu H, Yi L, Gao H, Deng X, et al. Reliability evaluation for WSNs based on deep reinforcement learning and graph neural networks. IEEE Trans Mob Comput. 2026;25(1):861–77. doi:10.1109/tmc.2025.3595199.
17. Natarajan VA, Kumar MS. Improving QoS in wireless sensor network routing using machine learning techniques. In: Proceedings of the 2023 International Conference on Networking and Communications (ICNWC); 2023 Apr 5–6; Chennai, India. New York, NY, USA: IEEE; 2023. p. 1–5. doi:10.1109/ICNWC57852.2023.10127349.

18. Tariq UU, Ali H, Hussain M, Liu L. Shuffled ARSH-FATI: a novel meta-heuristic for lifetime maximization of range-adjustable wireless sensor networks. IEEE Trans Green Commun Netw. 2023;7(3):1217–33. doi:10.1109/tgcn.2023.3278383.
19. Hiremani N, Basavaraju TG. Energy efficient routing protocols, classification and comparison in wireless sensor networks: a survey. In: Proceedings of the 2017 International Conference on Current Trends in Computer, Electrical, Electronics and Communication (CTCEEC); 2017 Sep 8–9; Mysore, India. New York, NY, USA: IEEE; 2018. p. 217–21. doi:10.1109/CTCEEC.2017.8455024.
20. Merabtine N, Djenouri D, Zegour DE. Towards energy efficient clustering in wireless sensor networks: a comprehensive review. IEEE Access. 2021;9:92688–705. doi:10.1109/ACCESS.2021.3092509.
21. Ali H, Tariq UU, Hussain M, Lu L, Panneerselvam J, Zhai X. ARSH-FATI: a novel metaheuristic for cluster head selection in wireless sensor networks. IEEE Syst J. 2021;15(2):2386–97. doi:10.1109/jsyst.2020.2986811.
22. Krishnakumar A, Anuratha V. Survey on energy efficient load-balanced clustering algorithm based on variable convergence time for wireless sensor networks. In: Proceedings of the 2016 3rd International Conference on Advanced Computing and Communication Systems (ICACCS); 2016 Jan 22–23; Coimbatore, India. New York, NY, USA: IEEE; 2016. p. 1–5. doi:10.1109/ICACCS.2016.7586361.
23. Heinzelman WR, Chandrakasan A, Balakrishnan H. Energy-efficient communication protocol for wireless microsensor networks. In: Proceedings of the 33rd Annual Hawaii International Conference on System Sciences; 2000 Jan 7; Maui, HI, USA. New York, NY, USA: IEEE; 2002. p. 10. doi:10.1109/HICSS.2000.926982.
24. Behera TM, Mohapatra SK, Samal UC, Khan MS, Daneshmand M, Gandomi AH. Residual energy-based cluster-head selection in WSNs for IoT application. IEEE Internet Things J. 2019;6(3):5132–9. doi:10.1109/jiot.2019.2897119.
25. Srinivasa Rao PC, Jana PK, Banka H. A particle swarm optimization based energy efficient cluster head selection algorithm for wireless sensor networks. Wirel Netw. 2017;23(7):2005–20. doi:10.1007/s11276-016-1270-7.
26. Loganathan S, Arumugam J. Energy efficient clustering algorithm based on particle swarm optimization technique for wireless sensor networks. Wirel Pers Commun. 2021;119(1):815–43. doi:10.1007/s11277-021-08239-z.
27. Liu Y, Huang H, Zhou J. A dual cluster head hierarchical routing protocol for wireless sensor networks based on hybrid swarm intelligence optimization. IEEE Internet Things J. 2024;11(9):16710–21. doi:10.1109/JIOT.2024.3355993.
28. Rezaeipanah A, Amiri P, Nazari H, Mojarad M, Parvin H. An energy-aware hybrid approach for wireless sensor networks using re-clustering-based multi-hop routing. Wirel Pers Commun. 2021;120(4):3293–314. doi:10.1007/s11277-021-08614-w.
29. Lin D, Min W, Xu J. An energy-saving routing integrated economic theory with compressive sensing to extend the lifespan of WSNs. IEEE Internet Things J. 2020;7(8):7636–47. doi:10.1109/JIOT.2020.2987354.